

## ABSTRACT

### INFLUENCE OF SMALL-SCALE CHEMICAL VARIATION OF SEDIMENT ON POSSIBLE METAMORPHIC ASSEMBLAGES

By

Donald Barker Seavey

Metamorphic petrology assumes a rather high level of homogeneity to the pre-metamorphic terrane. Failure of this assumption could lead to erroneous interpretations of the variations observed within a metamorphic complex.

Chemical and textural variations of a typical unmetamorphosed sedimentary basin have been determined by x-ray fluorescence, x-ray microprobe, and thin section analysis. The observed variations were then treated as a metamorphosed rock, were plotted on ACF, AFK and AFM diagrams, and the possible mineral assemblages were determined.

Sedimentary variations must become one of the factors that the metamorphic petrologist must consider when attempting to solve problems of metamorphic petrology if his solutions are not to be questioned.

INFLUENCE OF SMALL-SCALE CHEMICAL  
VARIATION OF SEDIMENT  
ON POSSIBLE METAMORPHIC ASSEMBLAGES

by

Donald Barker Seavey

A THESIS

Submitted to  
Michigan State University  
in partial fulfillment of the requirements  
for the degree of

MASTER OF SCIENCE

Department of Geology

1971

TABLE OF CONTENTS

ACKNOWLEDGEMENTS

The author wishes to express his appreciation to Professors Thomas A. Vogel, Robert Ehrlich, and Charles M. Spooner for their help and guidance in the writing of this thesis.

He also wishes to thank the Department of Geology of Michigan State University for the use of its equipment in conducting his research. A word of thanks is also due Mrs. Orlane Seavey for typing this manuscript; and last, but not least, special recognition is due his wife for her patience and understanding while he was preparing this thesis.

LIST OF TABLES

TABLE OF CONTENTS

	Page
INTRODUCTION .....	1
PURPOSE .....	2
PROCEDURE .....	5
Sample Collection .....	5
Sample Analysis .....	5
Sedimentary Petrography.....	7
The Metamorphic Model .....	12
Discussion of the Metamorphic Model.....	17
Granulite Facies .....	23
CONCLUSIONS .....	25
BIBLIOGRAPHY .....	30
APPENDIX I: SAMPLE PREPARATION .....	32
APPENDIX II: SEDIMENT DATA.....	34
APPENDIX III: X-RAY MICROPROBE DATA .....	46
APPENDIX IV: X-RAY FLUORESCENCE DATA .....	54

## LIST OF TABLES

TABLE 1:	ANALYSIS RESULTS .....	6
TABLE 2:	ASSEMBLAGE FREQUENCY TABLE ..... FOR THE GREENSCHIST FACIES ASSEMBLAGES	19
TABLE 3:	ASSEMBLAGE FREQUENCY TABLE ..... FOR THE ALMANDINE - AMPHIBOLITE FACIES ASSEMBLAGES	22
TABLE 4:	ASSEMBLAGE FREQUENCY TABLE ..... FOR THE GRANULITE FACIES ASSEMBLAGES	23

## TABLE OF FIGURES

	Page
Figure 1: LOCATION MAP OF SAMPLE SITE .....	3
Figure 2: SAMPLE COLLECTION SITE .....	4
Figure 3: FELDSPAR AND QUARTZ VS. $\Phi$ .....	8
Figure 4: PERCENT MATRIX AND OXIDES OF K, .....	9
Na, AND Al VS. DISTANCE (Samples A - H)	
Figure 5: PERCENT MATRIX AND OXIDES OF K, .....	10
Na, AND Al VS. DISTANCE (Samples 1 - 10)	
Figure 6: STRATIGRAPHIC COLUMN .....	11
Figure 7: COMPOSITION POINT OF SAMPLE E .....	14
WITHIN THE ALMANDINE-AMPHIBOLITE FACIES	
Figure 8: GREENSCHIST FACIES .....	18
Figure 9: ALMANDINE-AMPHIBOLITE FACIES .....	21
Figure 10: GRANULITE FACIES .....	24

## INTRODUCTION

Metamorphic petrology attempts to unravel past events and processes which have affected a particular metamorphosed rock or metamorphic complex. One approach to understanding the metamorphic process has been by experimental investigation of the response of various compositional varieties to pressure, temperature, and chemical environment. Another approach has been to observe mineralogical and geochemical changes in the field; and from these observations determine the pressure and temperature fields involved, and to some degree, separate the observed variation into a component due to metamorphic process and a component arising from patterns of variability inherent in the pre-metamorphosed terrane. Both field and laboratory studies have assumed a rather high level of geochemical homogeneity to the pre-metamorphic terrane. Failure of this assumption could lead to erroneous interpretation of the variations observed within a metamorphic complex. The place to begin an evaluation of this assumption of uniformity is in a volume of sedimentary rock no larger than a small outcrop in a metamorphic terrane. If the assumption must be modified at this scale, the assumption must be suspect at all greater scales.

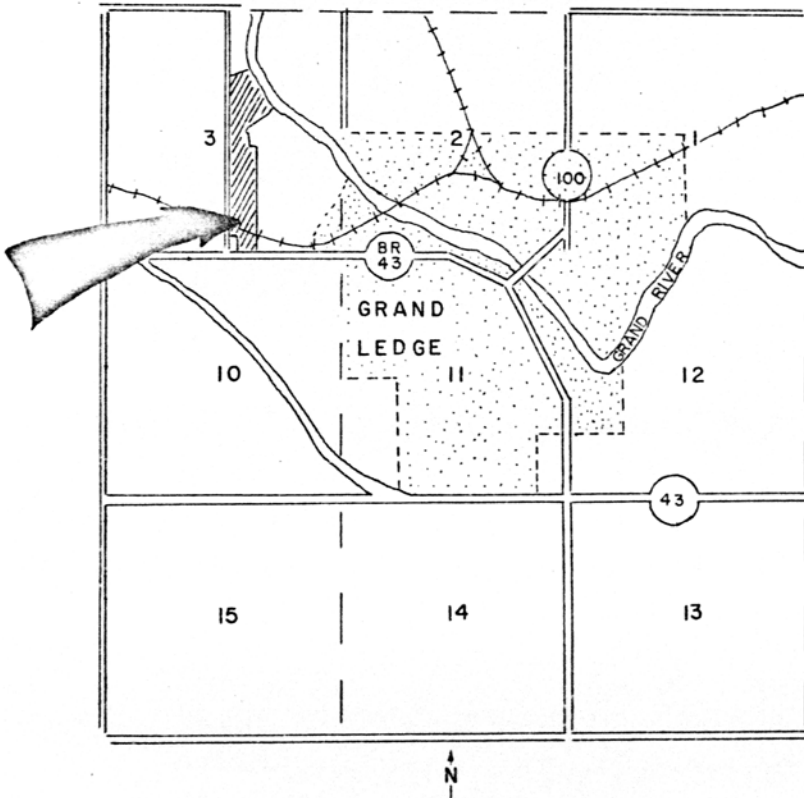
## PURPOSE

This study proposes to determine the variation, both chemical and textural, in a very small volume of unmetamorphosed sedimentary rock, and to simulate a range of metamorphic events on that material. The theoretical response will be examined in light of common assumptions in metamorphic studies.

Lower Pennsylvanian sedimentary rocks were collected from a quarry operated by the Grand Ledge Clay Tile Products Company near Grand Ledge, Michigan (Fig. 1). Aside from the fact that they are dominantly fine grained, these rocks have no special compositional qualities that enhance their worth as raw material for manufacture of drain tile. Indeed, these sandy shales are used as adulterant for quality control purposes to the output from another quarry. The outcrops were selected for this study because they represent a typical marine-deltaic environment which is common throughout the geologic column.

The samples were collected from a vertical interval of less than fifty feet and represent a duration of deposition of probably less than two hundred years. Compositional variations observed in these sediments arise only from geochemical variations within a depositional environment and the ever-present relation between size and composition. Samples were collected from two outcrops which represent lagoonal environments behind a barrier island.

Figure 1



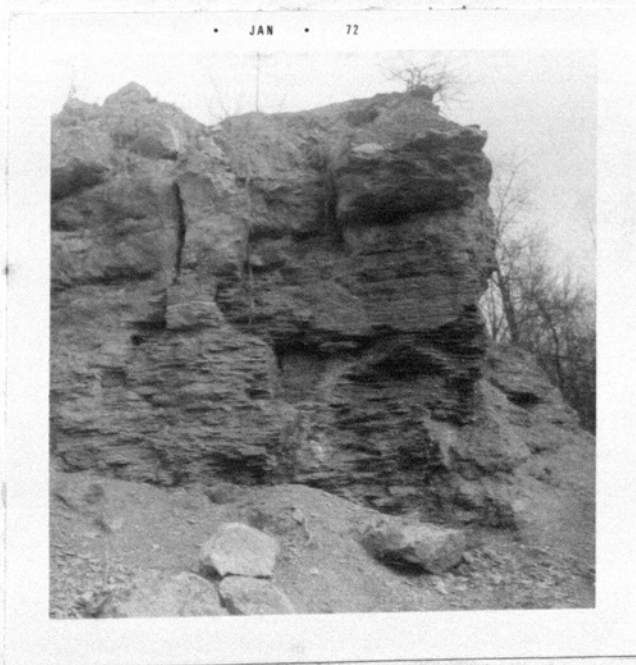
Quarry Location (Arrow) SW, SE Sec. 3 T4N, R4W

LOCATION MAP OF SAMPLE SITE

Figure 2



OUTCROP NO. 1: Samples A - H



OUTCROP NO. 2: Samples 1 - 10

## PROCEDURE

### Sample Collection:

Because this study had as its purpose the investigation of the range of response of a sedimentary volume to metamorphic events, samples were collected to obtain the widest spectrum of compositional variation. Eight samples were taken from the first outcrop, which is situated stratigraphically below the second outcrop. These samples (A through H) are predominately shales and siltstones. Ten samples (1 through 10) were collected from the second outcrop which grades upwards fairly continuously from fine shale to fine sandstone. Samples 11 and 11A were taken from sandstone capping the second outcrop. Sample 12, a black fissile shale, came from the drainage ditch situated both areally and stratigraphically between Outcrop 1 and Outcrop 2 and represents a very organically rich lagoonal bottom sediment (Fig. 2).

### Sample Analysis:

The chemical analysis of the samples was obtained by a modified version of the heavy absorber method of X-ray fluorescence as described by Rose et al. (1962). The same pellets used for X-ray fluorescence were also used for X-ray microprobe analyses. These methods were selected because of the advantages they offer: non-destructive to the samples; accuracy and precision; and time involved for preparation and analysis.



The samples were subjected to fluorescence long enough so that the accumulated counts would give an error of less than 2 percent at the 3 $\sigma$  confidence limit. The raw data was then compared to standards, and the mole percentages of the primary oxides were determined.

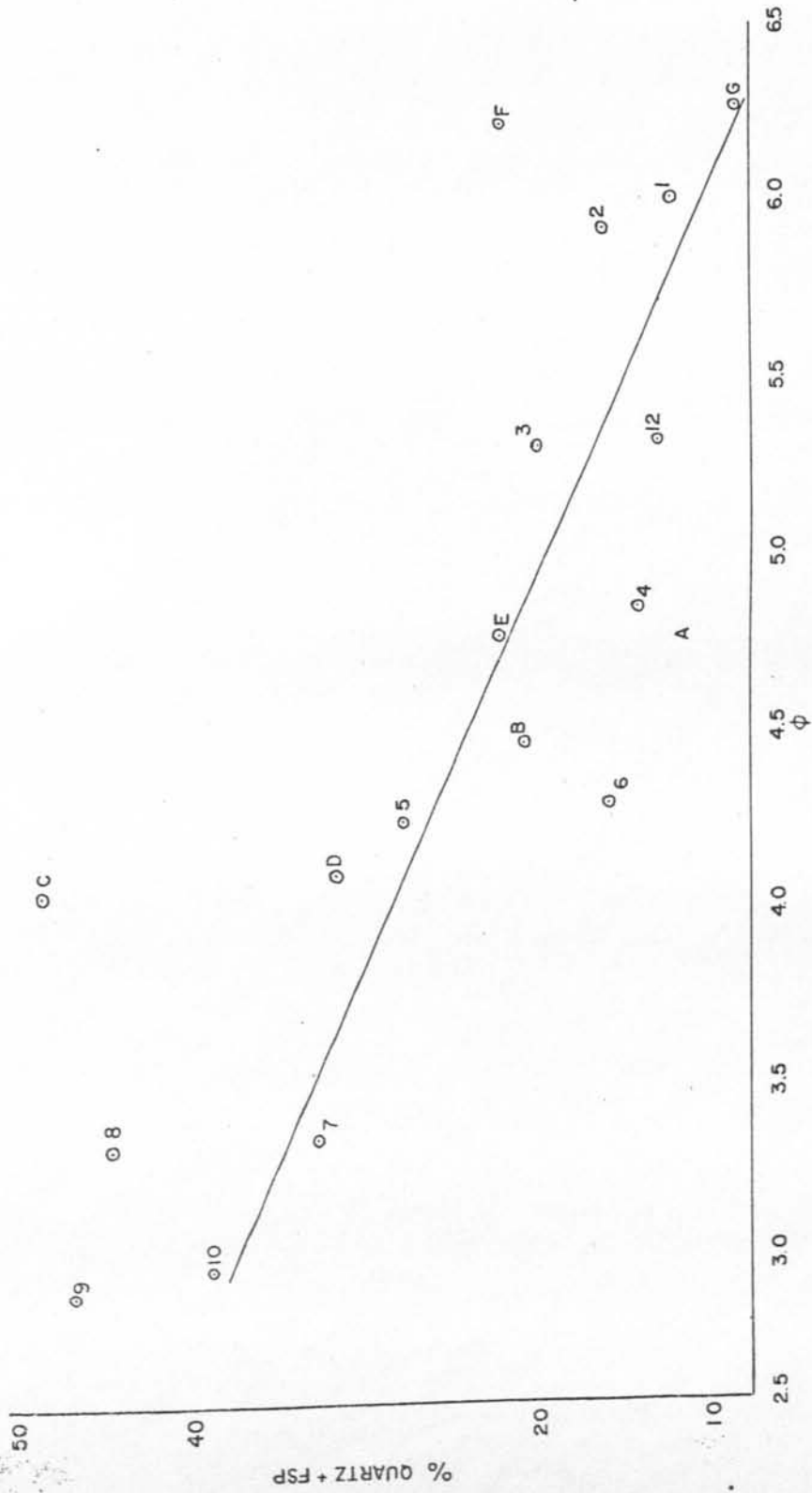
The major source of error within the analysis is attributed to the proportion of SiO<sub>2</sub> since it is the most abundant oxide present. This should not affect the hypothesized mineral assemblages, since quartz is not represented on the diagrams from which the metamorphic mineral assemblages are determined.

#### Sedimentary Petrography:

Thin sections were made of each sample and, to aid in distinction between quartz and feldspar, the sections were etched with hydrofluoric acid vapor for thirty seconds. Even with this, distinction between the two minerals in the finest grained samples was impossible. In those coarser grained sections in which the quartz and feldspar could be distinguished, modal proportions of quartz, feldspar and matrix were determined. Where the quartz and feldspar could not be differentiated, the point count was between the matrix and quartz plus feldspar. Relative grain size was estimated by measurement of the apparent long axis of the quartz grains.

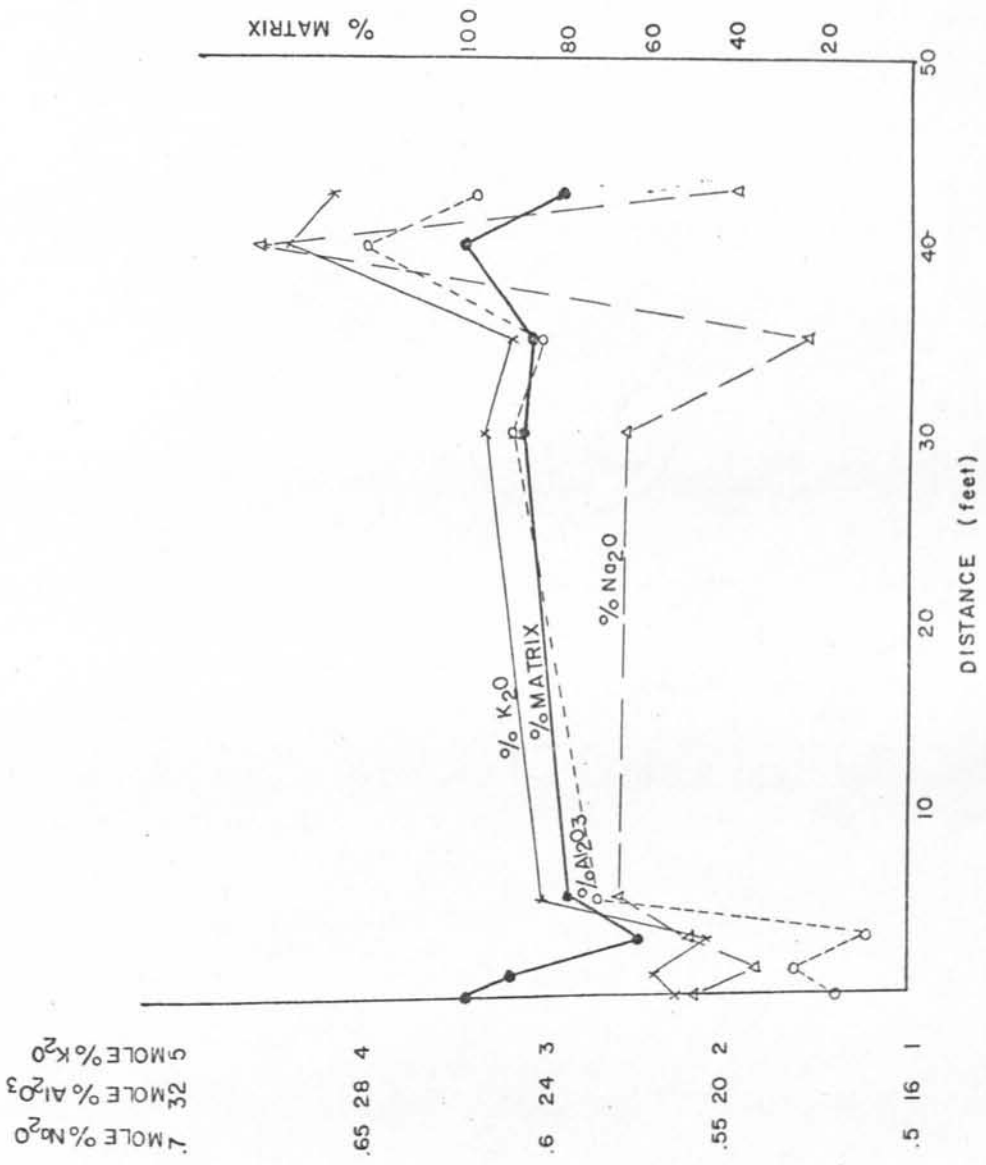
The results of this work indicate, as would be expected, that the percentage of quartz increases as the grain size increases (Fig. 3). Some of the samples appear to be too quartzose for their grain size.

Figure 3



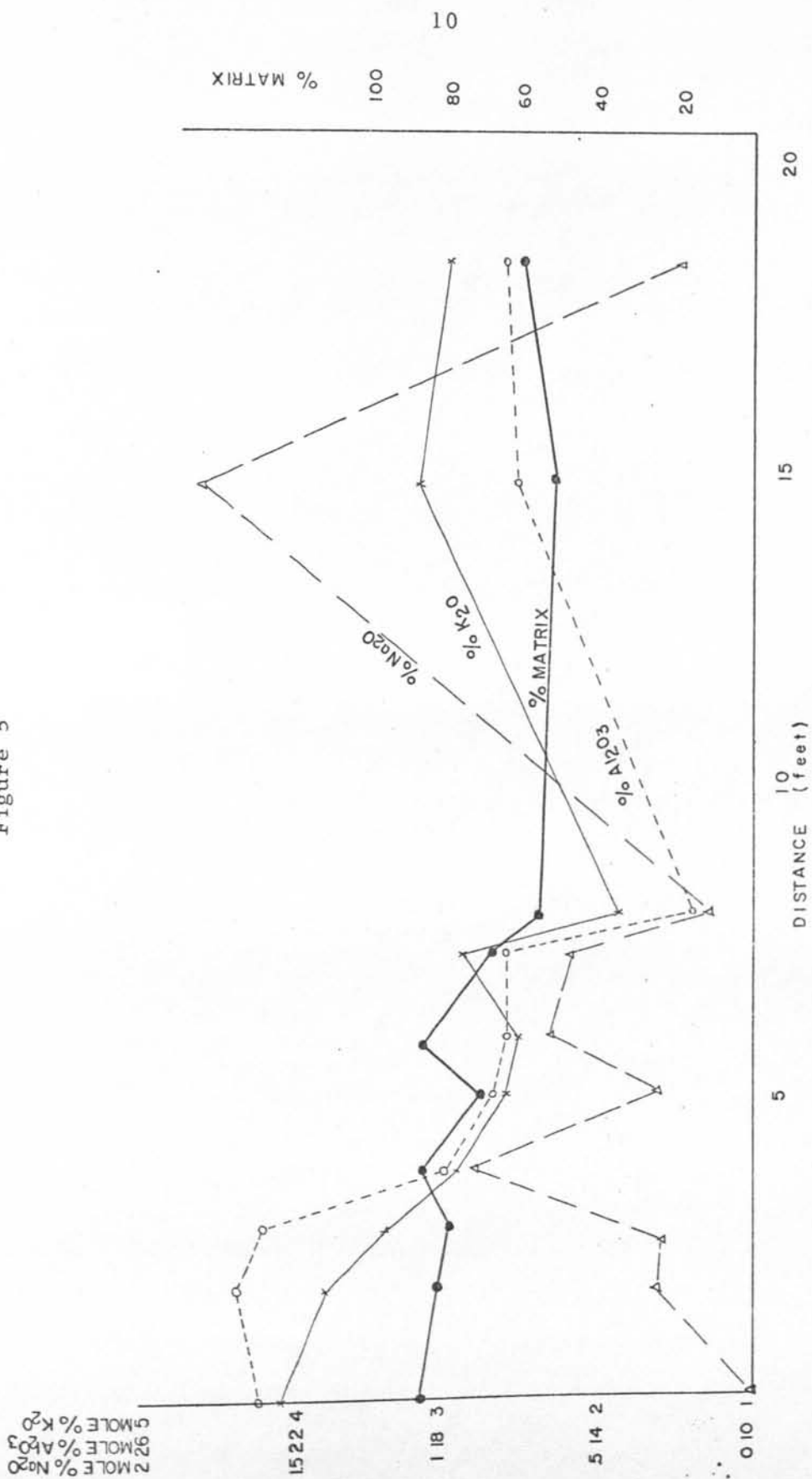
FELDSPAR AND QUARTZ VS.  $\phi$  (shows that quartz and feldspar content increases with grain size.  $\phi = -\log_2$  mm)

Figure 4



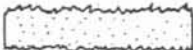
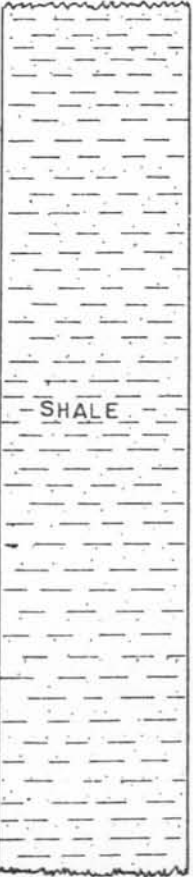
PERCENT MATRIX AND OXIDES OF K, Na, AND Al VS. DISTANCE (Samples A - H)

Figure 5



PERCENT MATRIX AND OXIDES OF K, Na, AND Al VS. DISTANCE (Samples 1 - 10)

Figure 6

Sample		$\phi$	%Qtz	Color	Lamina- tions
11		3.39	55	brownish grey	
10		3.09	23	lt. olive grey	yes
9		2.90	34	yellowish grey	
8		3.31	33	pale yellowish brown	
7		3.35	21	lt. olive	
6		4.30	12	drk. yellowish brown	yes
5		4.25	25	lt. brownish grey	yes
4		4.86	14	lt. olive grey	yes
3		5.31	19	lt. olive grey	yes
2		5.95	15	brownish grey	yes
1		6.02	11	medium grey	
12		5.34	13	drk. grey	
H		5.35	28	medium grey	yes
G		5.30	8	medium grey	
F		6.27	22	medium grey	
E		4.77	19	medium lt. grey	
D		4.10	30	lt. grey	
C	4.04	48	lt. brownish grey	yes	
B	4.49	20	lt. olive grey		
A	4.74	11	lt. olive grey	yes	

STRATIGRAPHIC COLUMN

Samples 11, C, F, and H are quartz rich, indicating that factors other than grain size were the governing influence during the periods these samples were deposited. Sample 11 comes from the sandstone capping the second outcrop and is most probably a beach facies on the landward side of the lagoon. The other samples come from the first (lower) outcrop and are probably an offshore sand facies derived from the beach face. Therefore, differences in elemental abundances between samples simply arise from the grain size composition relationships or from depositional environmental factors. No variations in provenance or paleoclimatology need be invoked to explain those variations.

A comparison of the mole percentages of the oxides of potassium, sodium, and aluminium in Samples A through H (Outcrop 1) indicates that these oxides vary directly with matrix proportions (Fig. 4). This indicates that these oxides are proportionately associated to fine grained micaceous matrix material, rather than in feldspars, and would be readily available for metamorphic reactions. A similar pattern is apparent between the oxides in the second outcrop, but association with matrix proportions in that outcrop is not apparent (Fig. 5).

#### The Metamorphic Model:

The oxide percentages were recalculated (in the manner of Winkler, 1967) for presentation on the triangular ACF and A'FK

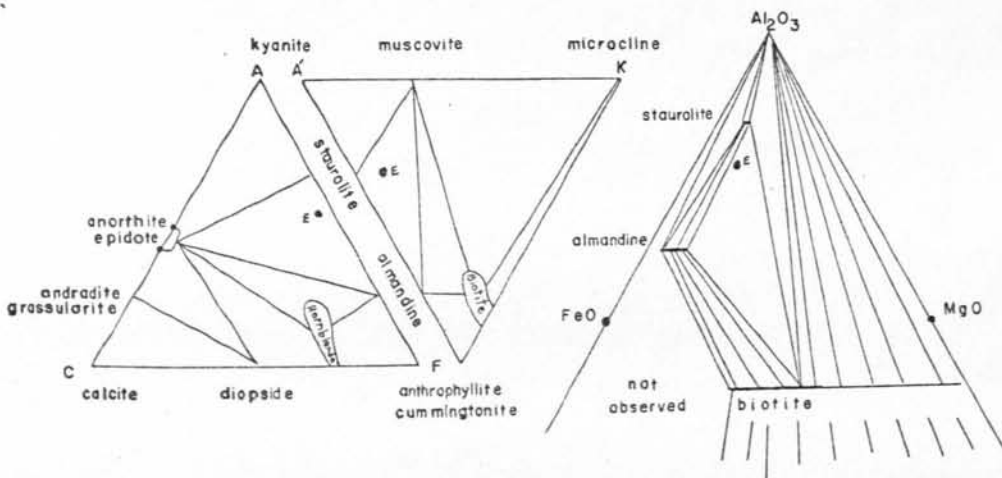
diagrams of Eskola (1939) and the AFM diagram of Thompson (1957). Consistent with other workers, several assumptions have been made in order to facilitate the calculations for the diagrams. First, all of the iron present has been assumed to be  $Fe^{++}$ , which may shift the composition point of the sample toward the F corner of the ACF diagram. Second, the water content of the samples has been ignored. Since most metamorphic reactions evolve water, the presence of a hydrous vapor phase is assumed. This would be especially true in rocks with a relatively high initial clay content. Third, little or no work has been done to relate such elements as carbon or sulfur to the metamorphic process, so they too have not been considered in the analysis.

The fundamental assumption made when using these diagrams is that the metamorphic process is isochemical and that the elements present in the original sediment remain. The minerals are just restructured, according to the conditions of equilibrium, into different mineral assemblages. In all cases equilibrium is assumed. This assumption is most valid for the finer grained rocks at the higher grades of metamorphism. This assumption is reasonable for rocks of this composition. The AFM diagrams also assume muscovite to be present in the assemblages. There is no composition point for sodium on the diagrams, and in these types of projections all sodium is assumed to be present as albite.

Some basic inferences about metamorphic textures have been made to relate the observed textures of the sediments to textures that might be expected upon metamorphism of the rock. The rocks with a high proportion of matrix to quartz and feldspar (about 60 to 70 percent matrix or more), would probably show a schistose texture, while those with high quartz plus feldspar content (greater than 40 percent) would probably have a granular or sugary texture. Interlayered and laminated sedimentary rocks within the samples may be reflected as gneissic textured metamorphic rocks.

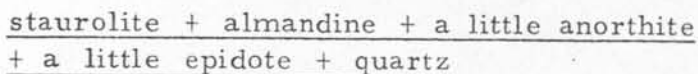
Fine grained crystals recrystallize earlier than coarser grained crystals during metamorphism. One might expect to find primary grains of quartz and feldspar in the coarser grained rocks at the lower grades of metamorphism.

Figure 7



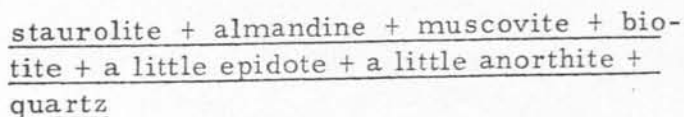
Composition point of Sample E within the Almandine-Amphibolite facies (after Winkler, 1967)

The point in the ACF diagram corresponding to the composition of Sample E falls within the subtriangle (anorthite, epidote)-staurolite-almandine, giving a preliminary assemblage of:



Since the composition point is close to the AF line, (low in CaO) the amount of anorthite and epidote would be limited. By the same reasoning the point is located closer to the staurolite point of the subtriangle than to the almandine point, so the composition includes more staurolite than almandine.

Consideration of the composition point in the A'FK diagram shows it to fall within the subtriangle staurolite-almandine-muscovite. The location of the point within the subtriangle indicates that there will be less muscovite than staurolite. When the Fe/Mg ratio, as represented by the AFM diagram, is considered, biotite will be added to the assemblage since the point falls within the composition field staurolite-almandine-biotite. The final assemblage will be:



This demonstrates the advantage of using the AFM diagram along with the ACF and A'FK diagrams. The FeO and MgO are not separated in the ACF and AFK diagrams, and it is not apparent that biotite coexists with staurolite. The AFM diagram shows the wide stability field of staurolite-almandine and biotite that is observed in metamorphic rocks.

The sample under consideration is a medium grained silty shale. The argillaceous matrix comprises 78 percent of the rock. Of the remaining 22 percent, 19 percent is quartz and 3 percent is feldspar. There are no observable laminations or other structures that might be preserved in the metamorphosed rock. Under the pressure and temperature expected in this metamorphic facies, it is probable that the rock would completely recrystallize with a schistose texture, and no primary crystals of quartz or feldspar would be present.

The ACF, A'FK and AFM diagrams on the following pages have been taken from Winkler (1967) and have been used as the basis for the determination of the mineral assemblages that would be expected in the various metamorphic facies.

The stratigraphic column (Fig. 6), derived from the information obtained by observation of the sediments, has been divided into the three major rock types present in the outcrops. The composition of the individual samples has been plotted on the ACF, A'FK and, where applicable, AFM diagrams. The upper diagrams represent the samples collected from the upper portion of the second outcrop and are sandstones. The center diagrams represent the siltstones from the middle portion of the second outcrop. Shales that comprise the entire first outcrop and the lower portion of the second outcrop are represented on the lower set of diagrams. The sample locations are numbered just to the right of the stratigraphic

column, and the plots of the particular samples are numbered on the diagrams in close proximity to the composition point of the sample.

#### Discussion of the Metamorphic Model:

The models discussed are based on three metamorphic facies. Within each of these metamorphic facies a variety of assemblages are present depending on the bulk composition of the rock. The facies presented are the greenschist facies, the almandine-amphibolite facies, and the granulite facies.

The greenschist facies represents the lower temperature grade of metamorphism. Within this facies the samples taken from the two outcrops will have the following assemblages (see Fig. 8).

1. pyrophyllite + epidote + chlorite + chloritoid + Muscovite + albite + quartz
2. epidote + chlorite + chloritoid + muscovite + albite + quartz
3. calcite + chlorite + microcline + epidote + stilpnomelane + quartz
4. calcite + chlorite + dolomite + microcline + stilpnomelane + albite + quartz
5. epidote + chloritoid + chlorite + muscovite + microcline + albite + quartz
6. pyrophyllite + chlorite + chloritoid + muscovite + albite + quartz
7. pyrophyllite + epidote + chlorite + chloritoid + muscovite + microcline + albite + quartz
8. microcline + muscovite + chlorite + chloritoid + albite + quartz

Figure 8

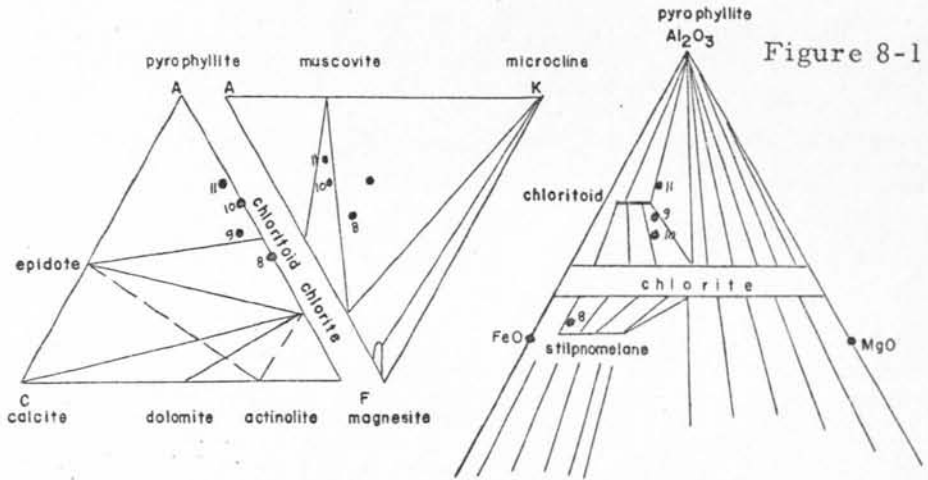
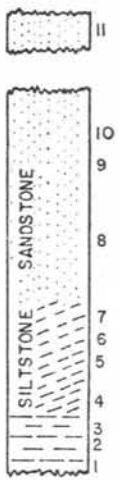


Figure 8-1

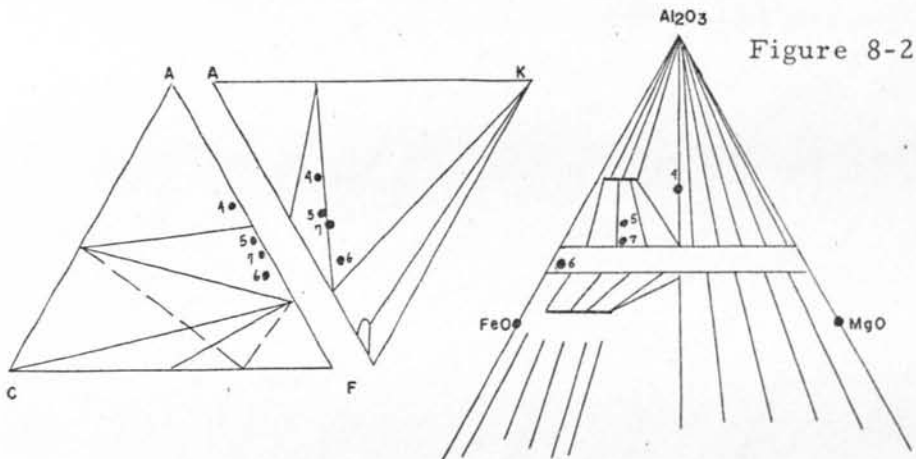
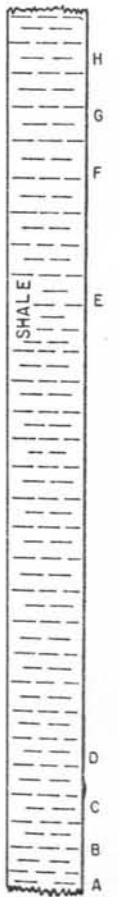


Figure 8-2

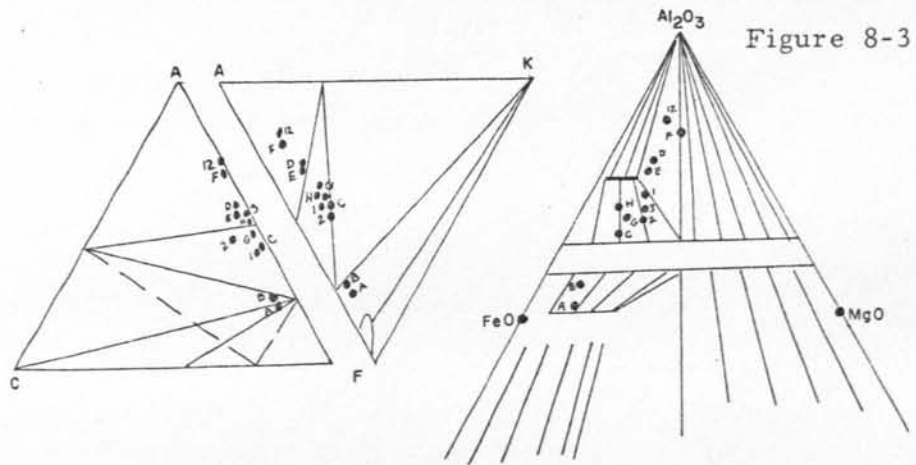


Figure 8-3

GREENSCHIST FACIES

The following table is based on the assemblages present in the greenschist facies. The assemblage number corresponds to the above numbered assemblages, the left-hand column refers to the part of the geologic column from which the sample comes, and the number within the table refers to the frequency that that assemblage appears.

TABLE 3  
ASSEMBLAGE FREQUENCY TABLE FOR  
THE GREENSCHIST FACIES ASSEMBLAGES

	1	2	3	4	5	6	7	8
Lower part of column	5	4	1	1		1		
Middle part of column	1	1			2			
Upper part of column	1					1	1	1

It is apparent that the most abundant assemblages are epidote + chlorite + chloritoid + muscovite + albite + quartz and pyrophyllite + epidote + chloritoid + chlorite + muscovite + albite + quartz in the shales from the lower part of the column, and epidote + pyrophyllite + chlorite + chloritoid + muscovite + albite + quartz in the middle and upper parts of the column. The amount of albite and epidote will be minor in all cases due to the limited amounts of CaO and Na<sub>2</sub>O in the bulk compositions of the rocks.

In the greenschist facies it might be noticed, from the AFM diagram (Fig. 8-3) representing the shales of the lower part of the column, that there appears to be a general trend of increasing  $\text{Al}_2\text{O}_3$  as we progress up the outcrop. There also appears to be a slight increase in MgO, tending to move the composition point upward and toward the center of the diagram. This moves some of the samples from the two-mineral to the three-mineral field. Samples D, E, F, and 12, for example, plot within the three-mineral field of chlorite-chloritoid-pyrophyllite. Within this field the chlorite and chloritoid have a fixed composition. In contrast, Samples 1, 2, 3, C, G, and H are less rich in  $\text{Al}_2\text{O}_3$  and MgO. The composition points are located in a two-mineral field of chlorite and chloritoid in which the composition of the minerals varies as the bulk composition of the rock varies. Samples A and B react in a similar manner, but are within the field of chlorite and stilpnomelane. Both minerals have compositions that will vary continuously with the bulk composition of the rock.

The almandine-amphibolite facies (Fig. 9) represents an intermediate grade of metamorphism and is characterized by the presence of plagioclase containing at least 15 percent anorthite (Winkler, 1967). The staurolite-almandine subfacies is the lower temperature subfacies and is distinguished by the presence of staurolite.

Figure 9

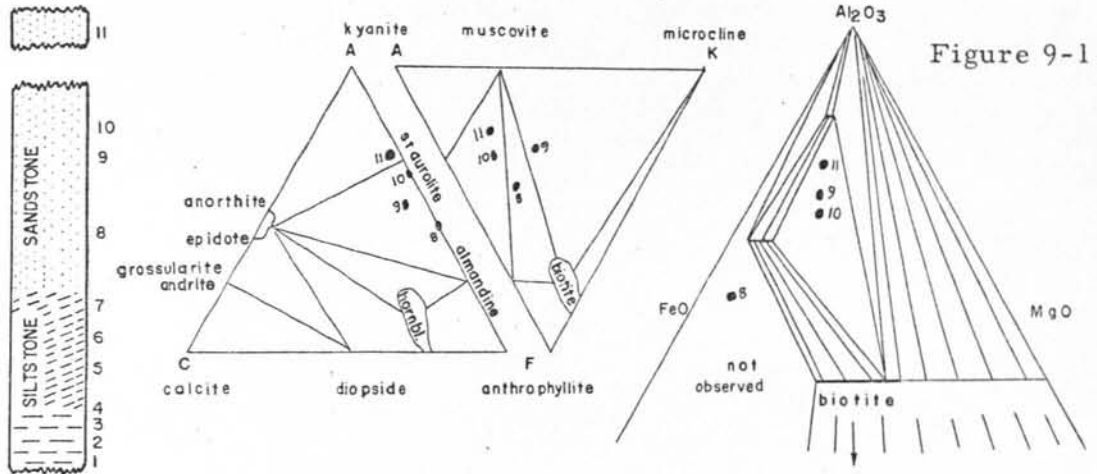


Figure 9-1

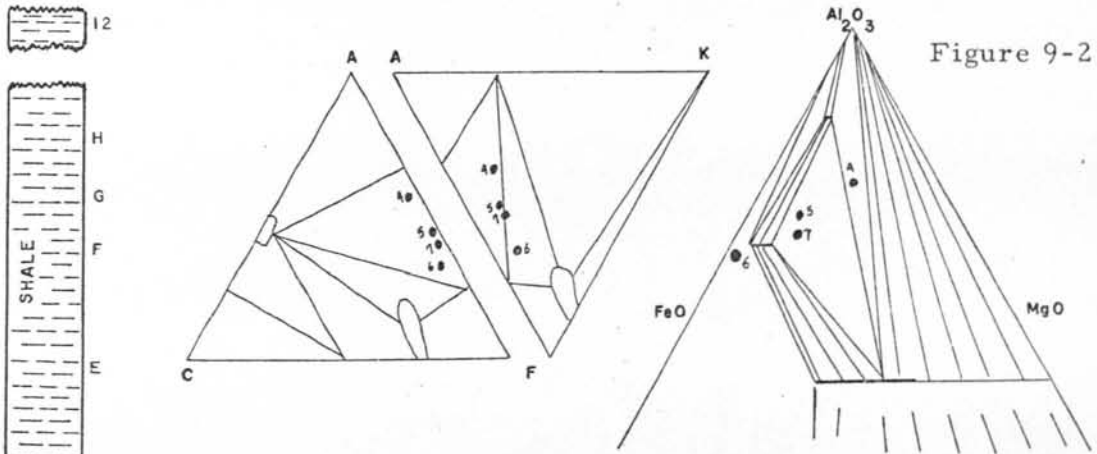


Figure 9-2

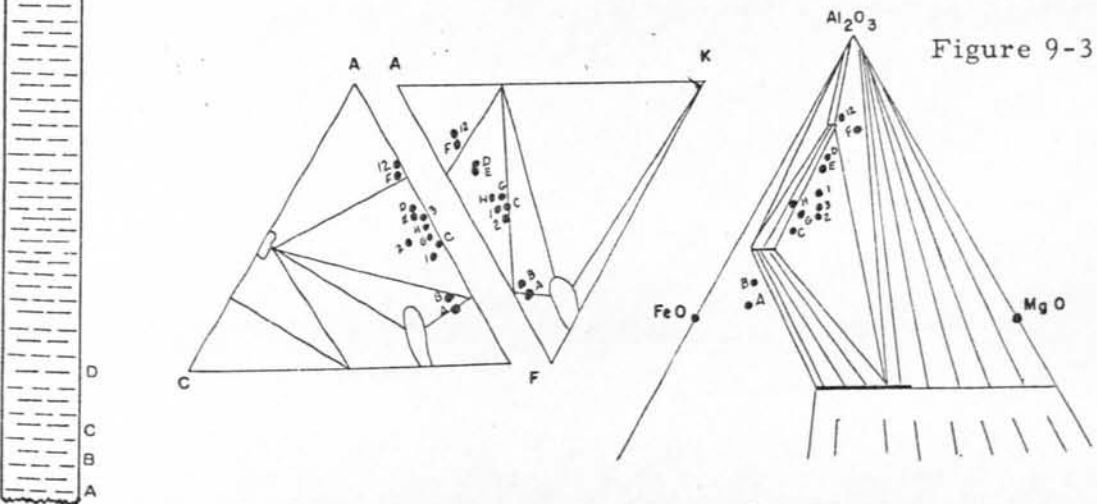


Figure 9-3

ALMANDINE-AMPHIBOLITE FACIES  
Staurolite-Almandine Subfacies

This facies would yield the following assemblages:

1. staurolite + almandine + plagioclase + epidote + biotite + muscovite + quartz
2. staurolite + almandine + plagioclase + epidote + kyanite + muscovite + biotite + quartz
3. staurolite + kyanite + muscovite + biotite + albite + almandine + quartz
4. almandine + hornblende + muscovite + plagioclase + epidote + biotite + quartz
5. staurolite + almandine + muscovite + biotite + albite + quartz
6. staurolite + almandine + plagioclase + epidote + microcline + muscovite + biotite + quartz

TABLE 3

ASSEMBLAGE FREQUENCY TABLE FOR THE  
ALMANDINE-AMPHIBOLITE FACIES ASSEMBLAGES

	1	2	3	4	5	6
Lower part of column	8	1	1	2		
Middle part of column	3	1				
Upper part of column		1			2	1

There is but one predominate assemblage in this facies, staurolite + almandine + muscovite + biotite + plagioclase + epidote + quartz. The plagioclase may or may not be present depending on whether there is any CaO present in the bulk composition.

Consideration of the AFM diagram of this facies (Fig. 9-3) indicates that most of the samples would form minerals of fixed composition. The exceptions are Samples A, B, H, 6, and 8. The composition of staurolite and almandine would vary with the bulk composition of the rock in Sample H. The other samples (A, B, 6, and 8) plot in a part of the diagram that is unobserved in metamorphic assemblages compiled by Winkler (1967).

#### Granulite Facies:

The granulite facies represents the high-rank metamorphic rocks. The column sampled can be represented in just four assemblages in this facies (Fig. 10).

1. kyanite + sillimanite + almandine + orthoclase + plagioclase + quartz
2. kyanite + almandine + sillimanite + orthoclase + ablite + quartz
3. kyanite + sillimanite + almandine + orthoclase + hypersthene + plagioclase + quartz
4. Hypersthene + almandine + orthoclase + quartz

TABLE 4

ASSEMBLAGE FREQUENCY TABLE FOR THE GRANULITE FACIES ASSEMBLAGES

	1	2	3	4
Lower part of column	9	1	1	1
Middle part of column	4			
Upper part of column	2	2		

Figure 10

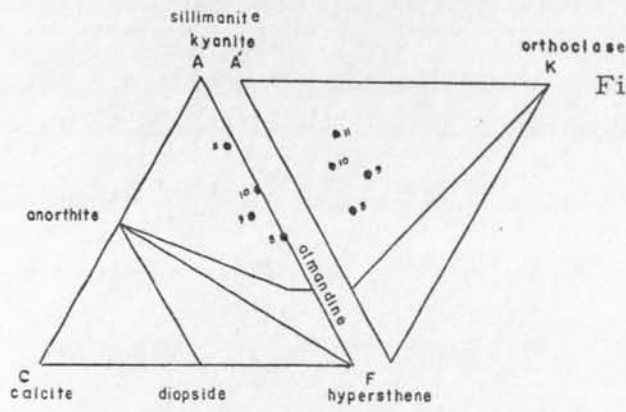
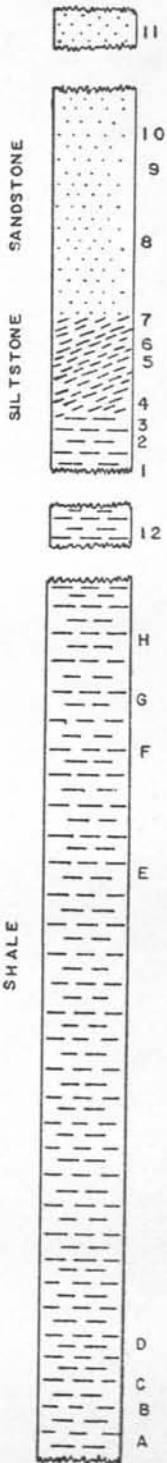


Figure 10-1

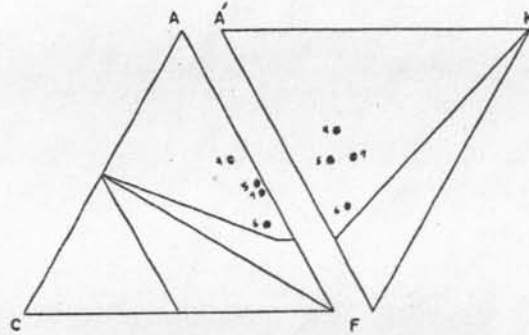


Figure 10-2

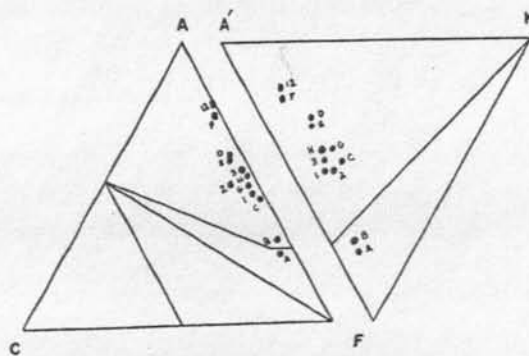


Figure 10-3

GRANULITE FACIES

The most abundant assemblage is kyanite + sillimanite + almandine + orthoclase  $\pm$  plagioclase  $\pm$  albite + quartz. The AFM diagram was not available for the granulite facies, so the mineral assemblages could well be incomplete.

With the exception of the shales in the greenschist facies, which had two predominate assemblages, the predominate assemblages in the shales, sandstones, and siltstones within a given facies are the same.

It becomes apparent that with increasing metamorphic grade the outcrop becomes more homogeneous in terms of mineral assemblages. From the greenschist facies, with two predominate assemblages in the shales, we move into but one assemblage in the almandine-amphibolite and the granulite facies.

## CONCLUSIONS

When attempting to solve metamorphic problems, the complexities and variations of the pre-existing sediments have not been fully considered. This study has attempted to relate the chemical and textural variations of an unmetamorphosed sediment to the spectrum of metamorphic mineral assemblages that would be formed from a given sedimentary environment under various conditions of metamorphism. To solve this problem, sediments from a tiny volume of a small marine-deltaic environmental complex has been analyzed. These facies are comparable to many such instances that are found

on a variety of scales throughout the geologic column, and the variations observed could thus occur over a much larger area. It should be emphasized that these sediments are not considered to be unusual in their genesis, compositional variety or depositional sequence.

This study shows that these facies, closely related in genetic process, and in time and space, exhibit complex patterns of chemical variation. Metamorphism of those variations will lead to a variety of metamorphic assemblages. This complexity is dominantly shown by the variation in alumina content. There is an overall tendency toward increased alumina content upward in the section (toward the beach facies). In contrast, the magnesia and iron oxide contents are relatively constant. Considerable variation is observed in each part of the section.

A striking feature that is brought out by this analysis is the common occurrence of the  $\text{Al}_2\text{SiO}_5$  minerals throughout the section, especially the presence of these minerals along with staurolite which greatly reduces the stability field of  $\text{Al}_2\text{SiO}_5$ . Many workers (i.e. Turner, 1968) have considered the presence of these  $\text{Al}_2\text{SiO}_5$  minerals to indicate a highly aluminous sediment. The analysis presented here indicates that these minerals would be present in typical marine-deltaic meta-sediments and that such assemblages as kyanite-staurolite bearing rocks interlayered with hornblende-almandine and staurolite-almandine bearing rocks might be expected (Fig. 9-3).

Primary textures may have an important role in determining the final metamorphic lithologies, especially in the lower grades of metamorphism. There is a general relationship of quartz and feldspar increasing with increasing grain size within a series of genetically related sediments (Fig. 3). A few of the samples are too quartz-feldspathic for their grain size. The coarser of these are probably beach deposits, while the finer grained samples may represent offshore fore-beach sands.

The effect of grain size on the metamorphic assemblages produced is twofold. First, the increase in grain size makes them less susceptible to recrystallization and primary textures are more likely to be preserved. Second, since the micaceous matrix minerals are affected more than the other phases, the quantitative increase of quartz and feldspar with grain size results in a smaller quantity of the minerals represented on the ACF, A'FK and AFM diagrams being formed. A certain amount of recrystallization of these minerals would be expected and would be necessary for the reactions to take place as predicted. The overall result would be the production of less schistose rocks (i.e. more granular) with increasing grain size. The finer grained samples that are too quartz-feldspathic should produce granular lithologies interlayered with the schistose ones which might be interpreted as being derived from a coarser grained sediment.

Since the mineral assemblages are independent of quartz content, the assemblages discussed above would occur at any and all grain sizes, assuming enough quartz recrystallizes to react. What would be represented here is a series of interlayered granulitic and schistose lithologies with a wide range of alumina contents. The quantities of the minerals formed from the oxides in feldspars would depend on the extent of recrystallization of the feldspar grains.

In the lower metamorphic grades (greenschist and staurolite-almandine subfacies of the almandine-amphibolite facies) the composition variation is cut by many tie lines. For example, in the ACF (Fig. 8-3 and Fig. 9-3) by chloritoid-epidote and staurolite-plagioclase and in the AFM by chloritoid-chlorite and staurolite-biotite tie lines. This in effect breaks the rock type into discreet assemblages. In the higher grades this compositional range is not transected because of the absence of the staurolite and chlorite fields.

This points out another important aspect of this study. If one of the goals of metamorphic petrology is to understand the variation of the premetamorphic rocks, then it can be seen that sampling becomes a critical problem. The chemical analysis of these sediments shows a nearly continuous variation with respect to alumina. If one samples an outcrop on the basis of mineral assemblages present in the granulite facies, a nearly complete spectrum could be obtained reflecting the true variation. If, however, in the greenschist facies one sampled on the same basis, two populations would

be obtained and erroneous conclusions would be made concerning the fundamental compositional variation of the metasediments. In order to obtain the true variation, the outcrop would have to be sampled in a random fashion.

A final result of this study is brought out by referring to the AFM diagram of the lower part of the section in the greenschist facies (Fig. 8-3). As has been discussed in detail above, some samples fall within the three-phase boundary field pyrophyllite-chloritoid-chlorite. In this field the compositions of all phases are invariant. Others fall in the two-phase field of chlorite and chloritoid, and in this field the composition of both of these phases is controlled by the bulk composition of the system. More importantly, however, is that the tie-lines showing the composition of chlorite and chloritoid are not parallel (Winkler, 1967). This means that the distribution of Fe and Mg between these two phases may change with bulk composition and that this distribution could not be used to determine variation in metamorphic conditions.

The importance of the original sedimentary variations must become one of the factors that the metamorphic petrologist considers when attempting to solve problems of metamorphic petrology if his solutions are not to be questioned.

## BIBLIOGRAPHY

- Barker, F., "Phase Relations in Cordierite-Garnet-Bearing Kinsman Quartz Monzonite and the Enclosing Schists, Lovewell Mountain Quadrangle, New Hampshire," American Mineralogist, Vol. 46 (1961), 1166-1176.
- Best, M. G. and Weiss, L. E., "Minerological Relations in some Pelitic Hornfelses From the Southern Sierra Nevada, California," American Mineralogist, Vol. 49 (1964), 1240-1266.
- Chinner, G. A., "Almandine in Thermal Aureoles," Journal of Petrology, Vol. 3 (1962), 316-340.
- Conolly, John R. and Ferm, John C., "Permo-Triassic Sedimentation Patterns, Sydney Basin, Australia," The American Association of Petroleum Geologists Bulletin, Vol. 55, No. 11 (November, 1971), 2018-2032.
- deWaard, D., "The Occurrence of Garnet in the Granulite-Facies Terrane of the Adirondack Highlands," Journal of Petrology, Vol. 6 (1965), 165-191.
- Ferm, John C., "Petrology of Some Pennsylvanian Sedimentary Rocks," Journal of Sedimentary Petrology, Vol. 32 (March 1962), 104-123.
- Gebhardt, Ronald F., "Principles of X-ray Spectroscopy: With Particular Reference to Light-Element Analysis," Department of Geological Engineering, (December, 1965).
- Griffiths, John C., Scientific Method in Analysis of Sediments, New York (1967).
- Spry, Alan, Metamorphic Textures, London (1969).
- Thompson, J. B., "The Graphical Analysis of Mineral Assemblages in Pelitic Schists," American Mineralogist, Vol. 42 (1957), 842-858.
- Turner, Francis J., Metamorphic Petrology, New York (1968).

Winkler, G. H. F., Petrogenesis of Metamorphic Rocks, New York (1967).

Zen, E-an, "Metamorphism of Lower Paleozoic Rocks in the Vicinity of the Taconic Range in West-Central Vermont, American Minerologist, Vol. 45 (1960), 129-175.

APPENDIX I

## SAMPLE PREPARATION

Each sample was first crushed so that it would pass through a 60- to 120-mesh screen. Next 100.0 mg of the sample, 100.0 mg of  $\text{La}_2\text{O}_3$ , and 700 mg of  $\text{Li}_2\text{B}_4\text{O}_7$  were weighed out on a piece of glassine paper. This was then poured into a polished agate mortar and mixed with a spatula. After being thoroughly mixed, all of the sample was transferred to a graphite crucible and placed in the furnace which was preheated to  $1050^\circ\text{C}$  and left for ten minutes. The bead formed was then placed on the balance and loose boric acid was added until the weight was brought up to 920 gm. The bead was then transferred to a grinding vial and shattered with a broad tipped punch. Then the boric acid was added and the whole mixture was pulverized in the Spex mixer with a tungsten carbide ball. It was left in the mixer for ten minutes. An aluminium cup was then filled with boric acid and compressed. The specimen powder was then placed in the center of the boric acid surface and spread evenly. Next, the cup was placed in the hydraulic press and placed under four tons p.s.i. for ten seconds. The resulting wafers were used for the X-ray fluorescence. They were then carbon coated for use on the X-ray probe.

APPENDIX II

OPTICAL EXAMINATION OF THIN  
SECTIONS

<u>Sample A</u>		<u>Objective 100x</u>	<u>Ocular 7x</u>	<u>Scope Units</u>	<u><math>\phi</math></u>
quartz	11%			17	4.87
feldspar	--			20	4.64
matrix	89%			5	6.64
$\phi$ av	4.74			24	4.38
				11	5.50
				20	4.64
				31	4.01
				25	4.32
				42	3.57
				30	4.85
<u>Sample B</u>		<u>Objective 100x</u>	<u>Ocular 7x</u>	<u>Scope Units</u>	<u><math>\phi</math></u>
quartz	20%			29	4.10
feldspar	1%			19	4.71
matrix	79%			14	5.15
$\phi$ av	4.49			20	4.64
				25	4.32
				39	3.68
				39	3.68
				12	5.38
				20	4.64
				20	4.64

<u>Sample C</u>		<u>Objective 100x</u>	<u>Ocular 7x</u>	<u>Scope Units</u>	<u><math>\phi</math></u>
quartz	48%			27	4.21
feldspar	1%			31	4.01
matrix	51%			30	4.05
$\phi$ av	4.04			50	3.32
				16	4.96
				31	4.01
				35	3.83
				37	3.75
				39	3.68
				20	4.64

<u>Sample D</u>		<u>Objective 100x</u>	<u>Ocular 7x</u>	<u>Scope Units</u>	<u><math>\phi</math></u>
quartz	30%			27	4.21
feldspar	2%			50	3.32
matrix	68%			47	3.41
$\phi$ av	4.10			28	4.15
				27	4.21
				23	4.44
				15	5.05
				29	4.10
				28	4.15
				30	4.05

<u>Sample E</u>		<u>Objective 100x</u>	<u>Ocular 7x</u>	<u>Scope Units</u>	<u><math>\phi</math></u>
quartz	19%			15	5.05
feldspar	3%			18	4.79
matrix	78%			27	4.21
$\phi$ av	4.77			12.5	5.31
				15	5.05
				30	4.05
				21	4.57
				19	4.71
				14	5.15
				17	4.87

<u>Sample F</u>		<u>Objective 100x</u>	<u>Ocular 7x</u>	<u>Scope Units</u>	<u><math>\phi</math></u>
quartz	22%			7	6.15
feldspar	--			7	6.15
matrix	78%			3	7.38
$\phi$ av	6.27			6	6.38
				7	6.15
				8	5.96
				8	5.96
				5	6.64
				7.5	6.15
				9	5.79

<u>Sample G</u>	<u>Objective 100x</u>	<u>Ocular 7x</u>	<u>Scope Units</u>	<u><math>\phi</math></u>
quartz	8%		3	7.38
feldspar	--		6	6.38
matrix	92%		8	5.96
$\phi$ av	6.30		4	6.96
			6	6.38
			7	6.15
			6	6.38
			10	5.64
			10	5.64
			7	6.15

<u>Sample H</u>	<u>Objective 100x</u>	<u>Ocular 7x</u>	<u>Scope Units</u>	<u><math>\phi</math></u>
quartz	28%		10	5.64
feldspar	1%		14	5.15
matrix	71%		11	5.50
$\phi$ av	5.35		9	5.79
			25	4.32
			6	6.38
			12	5.38
			16	4.96
			16	4.96
			11	5.50

<u>Sample 1</u>		<u>Objective 100x</u>	<u>Ocular 7x</u>	<u>Scope Units</u>	<u><math>\phi</math></u>
quartz	11%			6	6.38
feldspar	1%			15	4.05
matrix	88%			11	5.50
$\phi$ av	6.02			9	5.79
				5	6.64
				7	6.15
				6	6.38
				9	5.79
				5	6.64
				4	6.96

<u>Sample 2</u>		<u>Objective 100x</u>	<u>Ocular 7x</u>	<u>Scope Units</u>	<u><math>\phi</math></u>
quartz	15%			6	6.38
feldspar	1%			4	6.96
matrix	84%			5	6.64
$\phi$ av	5.95			7	6.15
				12	5.38
				12.5	5.31
				10	5.64
				25	4.32
				7	6.15
				5	6.64

<u>Sample 3</u>		<u>Objective 40x</u>	<u>Ocular 7x</u>	Scope Units	$\phi$
quartz	19%			2	6.33
feldspar	1%			5	5.95
matrix	80%			7	4.46
$\phi$ av	5.31			2	6.33
				3	5.75
				6	4.69
				10	3.94
				6	4.69
				2	6.33
				6	4.69

<u>Sample 4</u>		<u>Objective 40x</u>	<u>Ocular 7x</u>	Scope Units	$\phi$
quartz	14%			10	3.94
feldspar	2%			8	4.28
matrix	84%			5	5.95
$\phi$ av	4.86			7	4.46
				3	5.75
				7	4.46
				9	4.12
				3	5.75
				2	6.33
				9	4.12

<u>Sample 5</u>		<u>Objective 40x</u>	<u>Ocular 7x</u>	<u>Scope Units</u>	<u><math>\phi</math></u>
quartz	25%			3	5.75
feldspar	3%			3	5.75
matrix	72%			11	3.80
$\phi$ av	4.25			9	4.12
				11	3.80
				14	3.45
				18	3.04
				20	2.95
				10	3.94
				5	5.95

<u>Sample 6</u>		<u>Objective 40x</u>	<u>Ocular 7x</u>	<u>Scope Units</u>	<u><math>\phi</math></u>
quartz	12%			9	4.12
feldspar	4%			5	5.95
matrix	84%			10	3.94
$\phi$ av	4.30			7	4.46
				8	4.28
				11	3.78
				12	3.64
				7	4.46
				10	3.94
				7	4.46

<u>Sample 7</u>		<u>Objective 40x</u>	<u>Ocular 7x</u>	<u>Scope Units</u>	<u><math>\phi</math></u>
quartz	21%			12	3.68
feldspar	12%			20	2.95
matrix	67%			22	2.81
$\phi$ av	3.35			17	3.18
				14	3.45
				10	3.94
				16	3.27
				10	3.94
				11	3.78
				27	2.51

<u>Sample 8</u>		<u>Objective 20x</u>	<u>Ocular 7x</u>	<u>Scope Units</u>	<u><math>\phi</math></u>
quartz	33%			9	3.47
feldspar	12%			10	3.32
matrix	57%			8	3.64
$\phi$ av	3.31			15	2.74
				12	3.06
				13	2.95
				7	3.84
				11	3.18
				8	3.64
				10	3.32

<u>Sample 9</u>		<u>Objective 20x</u>	<u>Ocular 7x</u>	<u>Scope Units</u>	<u><math>\phi</math></u>
quartz	34%			6	4.06
feldspar	13%			8	3.64
matrix	53%			15	2.74
$\phi$ av	2.90			19	2.40
				13	2.95
				15	2.74
				25	2.00
				13	2.48
				10	3.32
				15	2.74

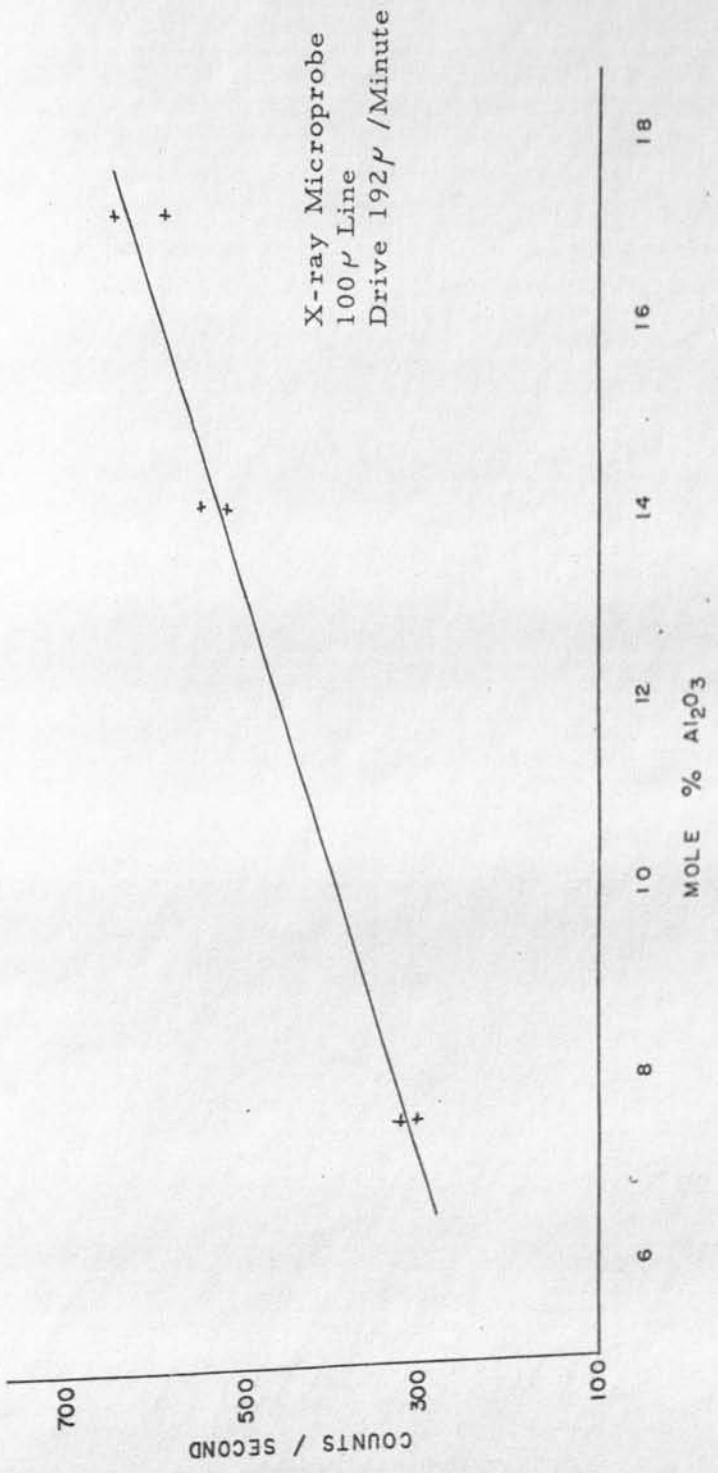
<u>Sample 10</u>		<u>Objective 20x</u>	<u>Ocular 7x</u>	<u>Scope Units</u>	<u><math>\phi</math></u>
quartz	23%			12	3.06
feldspar	16%			18	2.48
matrix	62%			17	2.56
$\phi$ av	3.09			13	2.95
				9	3.47
				14	2.84
				15	2.74
				6	4.06
				10	3.32
				9	3.47

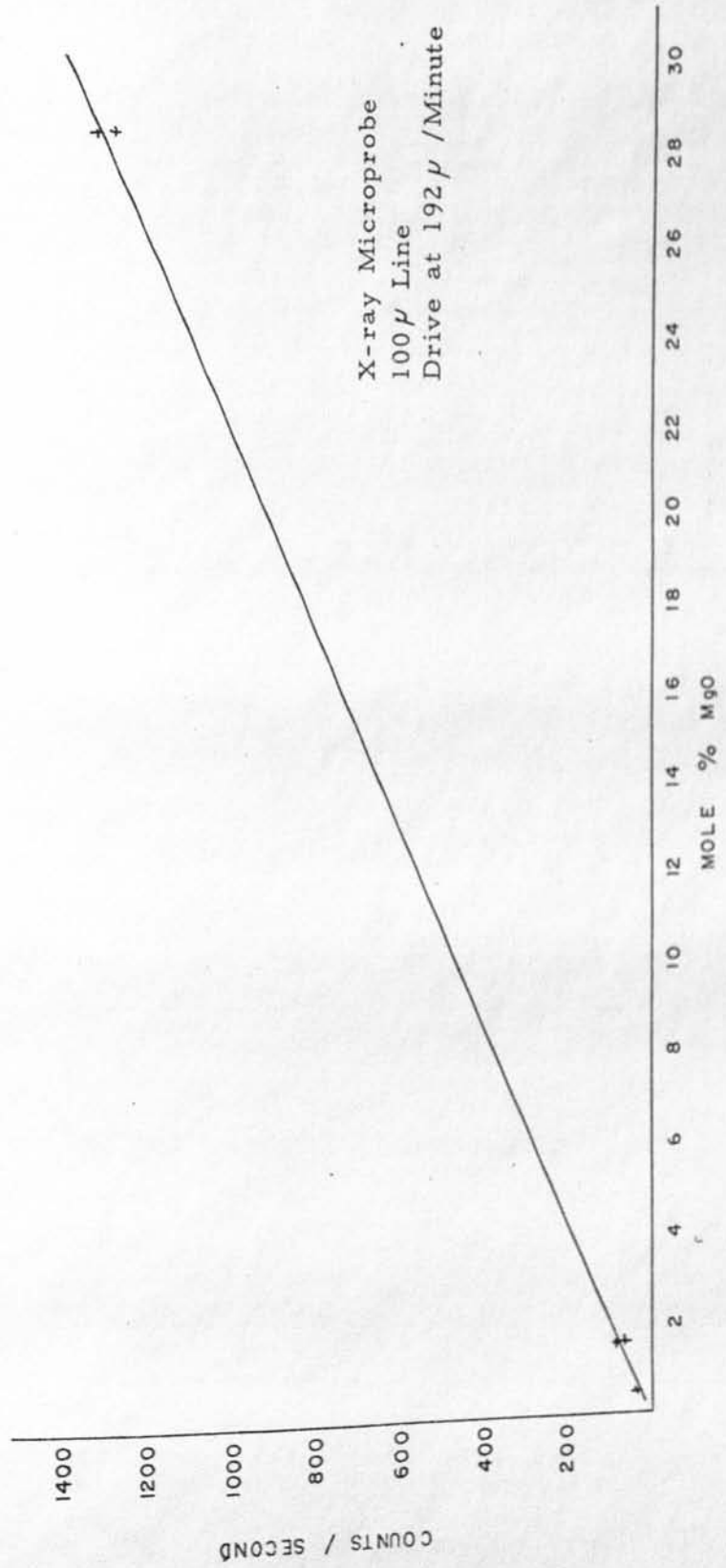
<u>Sample 11</u>		<u>Objective 20x</u>	<u>Ocular 7x</u>	<u>Scope Units</u>	<u><math>\phi</math></u>
quartz	55%			9	3.47
feldspar	12%			11	3.18
matrix	33%			15	2.74
$\phi$ av	3.39			4	4.66
				14	2.84
				11	3.18
				8	3.64
				15	2.74
				8	3.64
				7	3.84

<u>Sample 11A</u>		<u>Objective 40x</u>	<u>Ocular 7x</u>	<u>Scope Units</u>	<u><math>\phi</math></u>
quartz	30%			19	2.89
feldspar	5%			31	2.31
matrix	65%			14	3.45
$\phi$ av	3.12			7	4.46
				28	2.47
				20	2.95
				16	3.27
				24	2.68
				16	3.27
				14	3.45

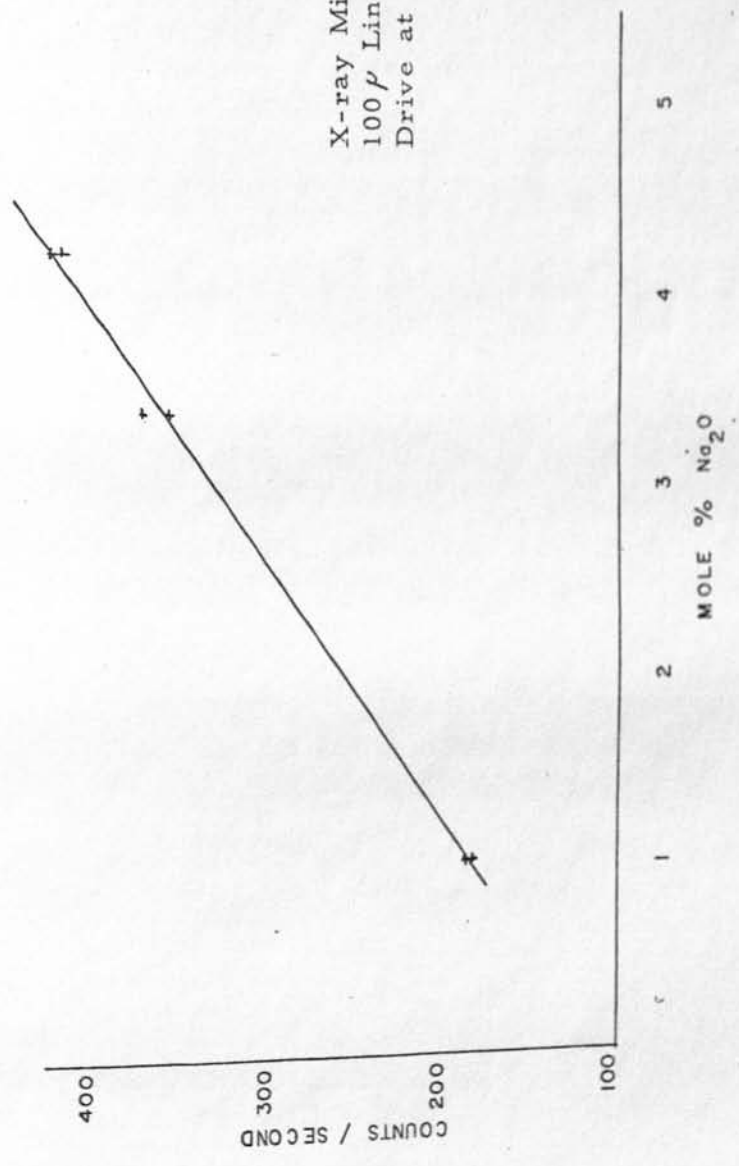
<u>Sample 12</u>	<u>Objective 100x</u>	<u>Ocular 7x</u>	<u>Scope Units</u>	<u><math>\phi</math></u>
quartz	13%		14	5.15
feldspar	--		10	5.64
matrix	87%		10	5.64
$\phi$ av	5.34		17	4.87
			13	5.26
			12	5.38
			20	5.64
			13	5.26
			13	5.26
			12	5.38

APPENDIX III





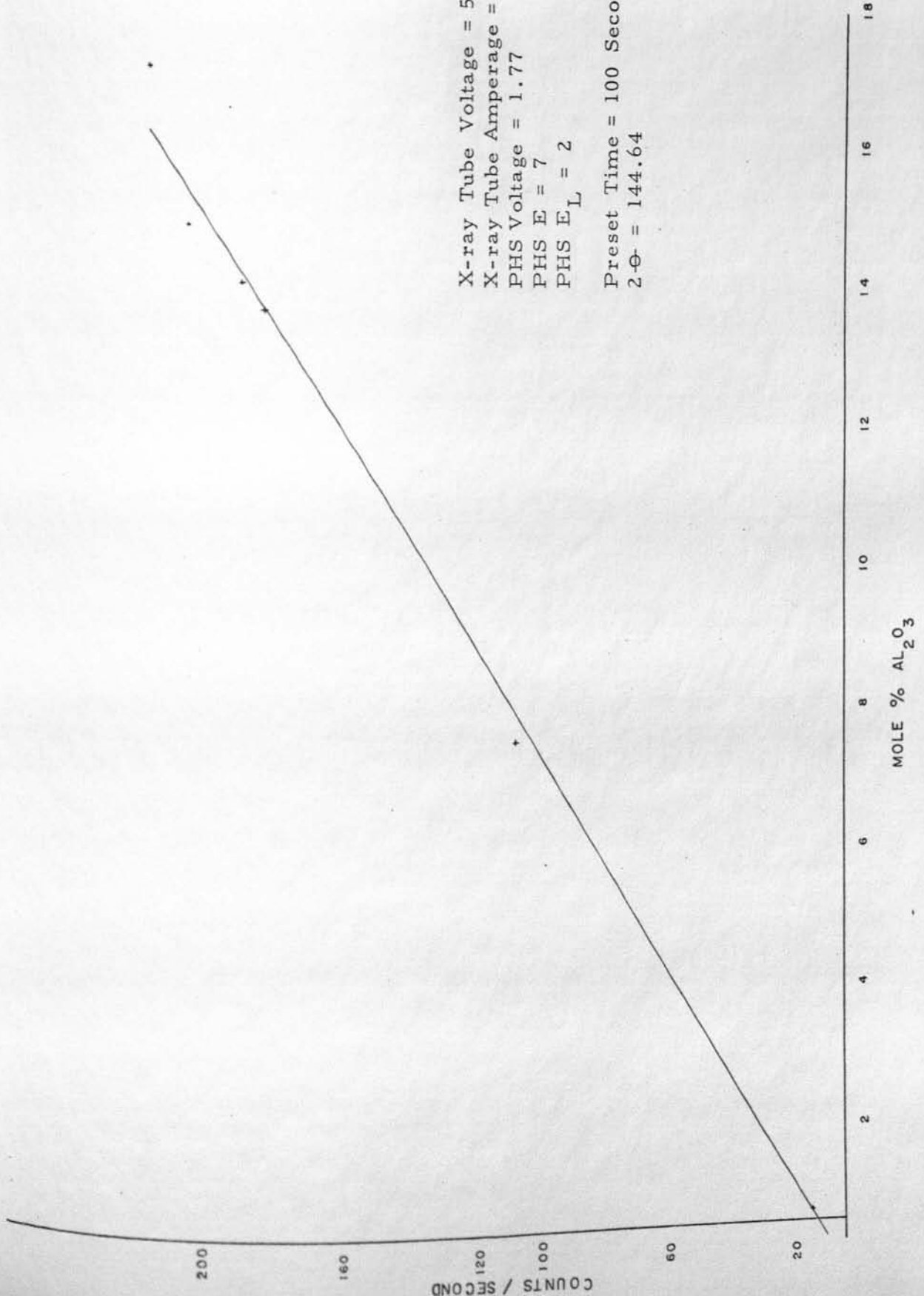
X-ray Microprobe  
100  $\mu$  Line  
Drive at 192  $\mu$  /Minute



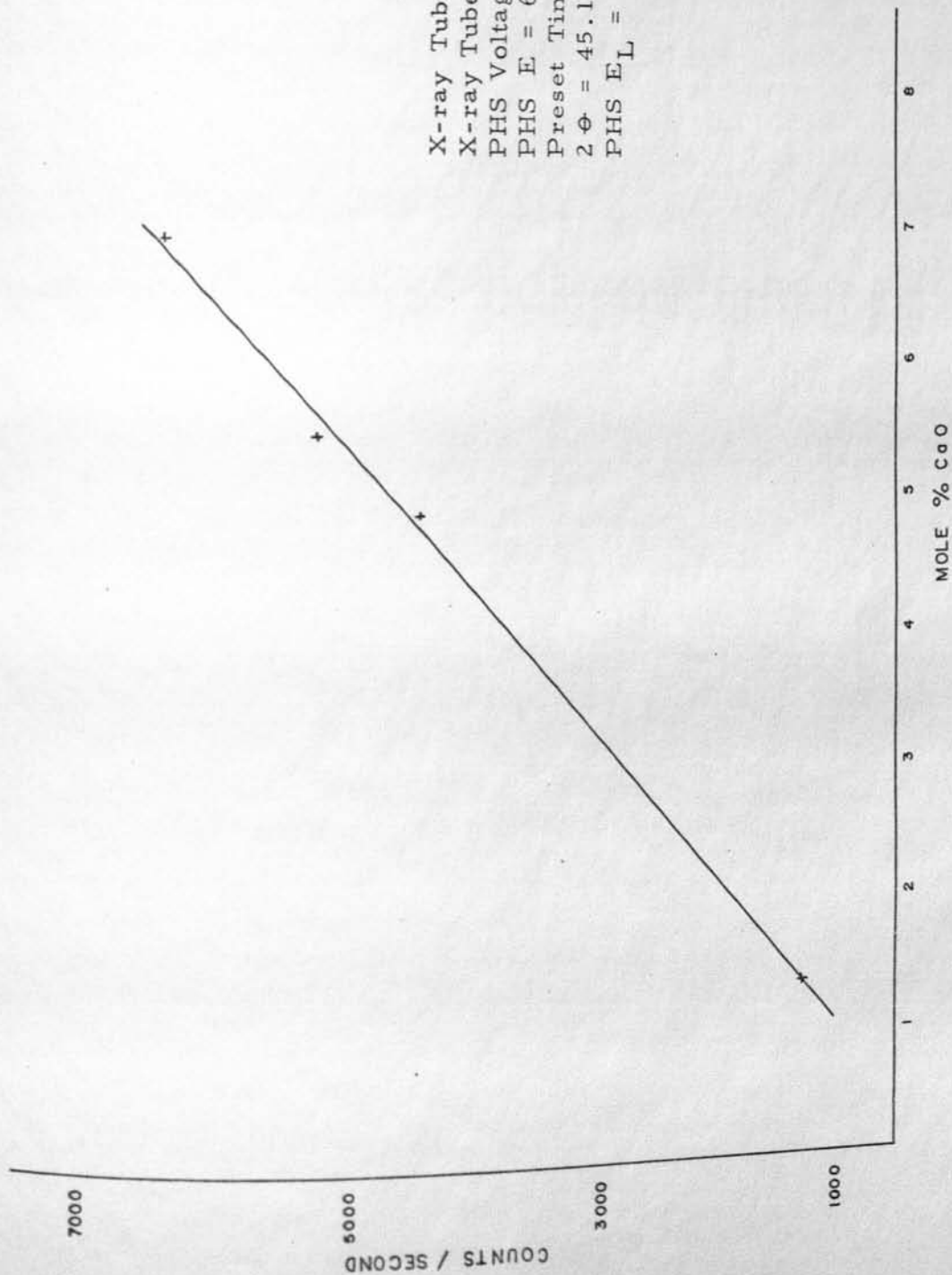
APPENDIX IV

X-ray Tube Voltage = 50 KV  
X-ray Tube Amperage = 50 MA  
PHS Voltage = 1.77  
PHS E = 7  
PHS E<sub>L</sub> = 2

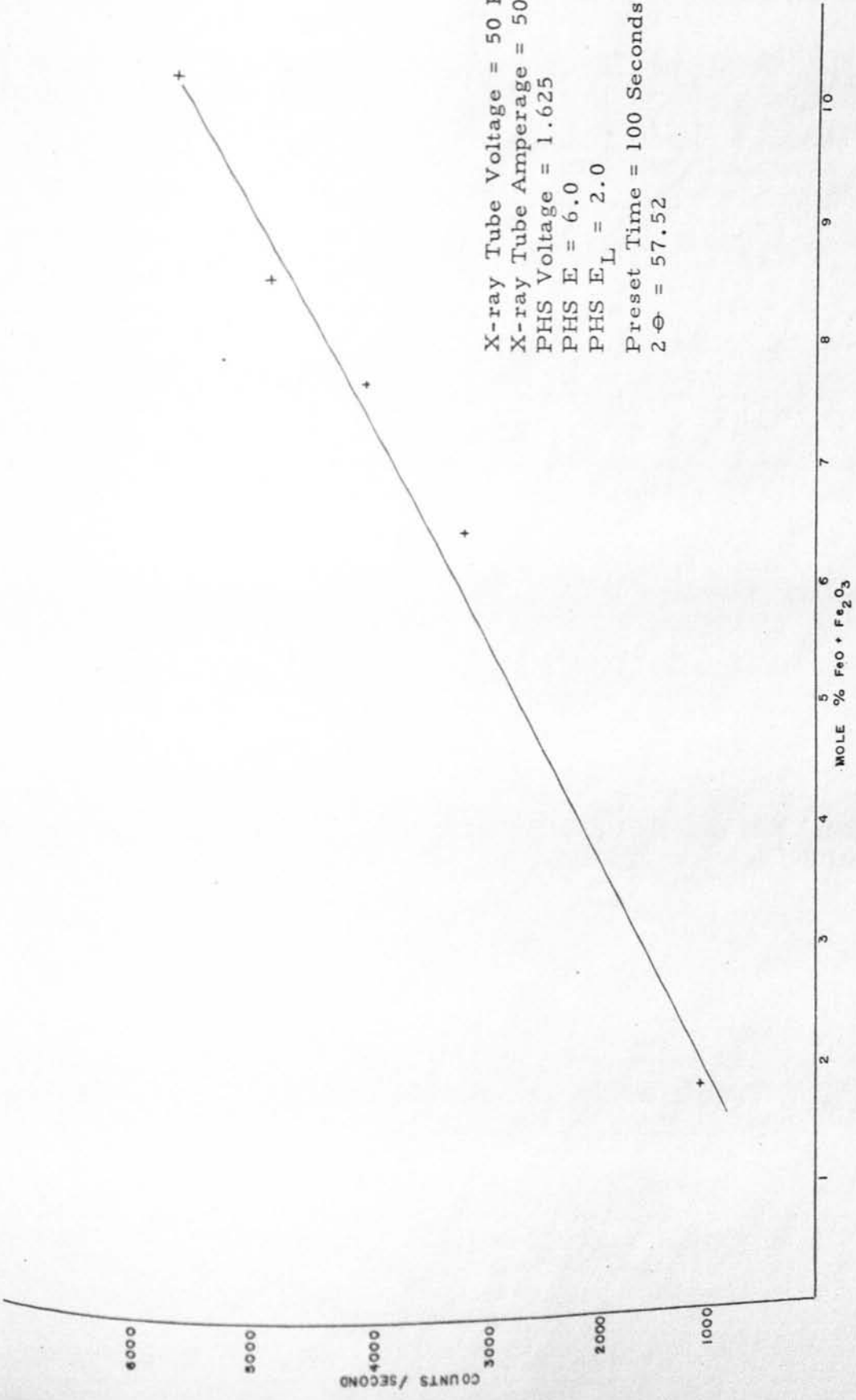
Preset Time = 100 Seconds  
2- $\theta$  = 144.64



X-ray Tube Voltage = 60 KV  
X-ray Tube Amperage = 50 MA  
PHS Voltage = 1.6 KV  
PHS E = 6  
Preset Time = 100 Seconds  
 $2\theta = 45.15$   
PHS  $E_L = .5$

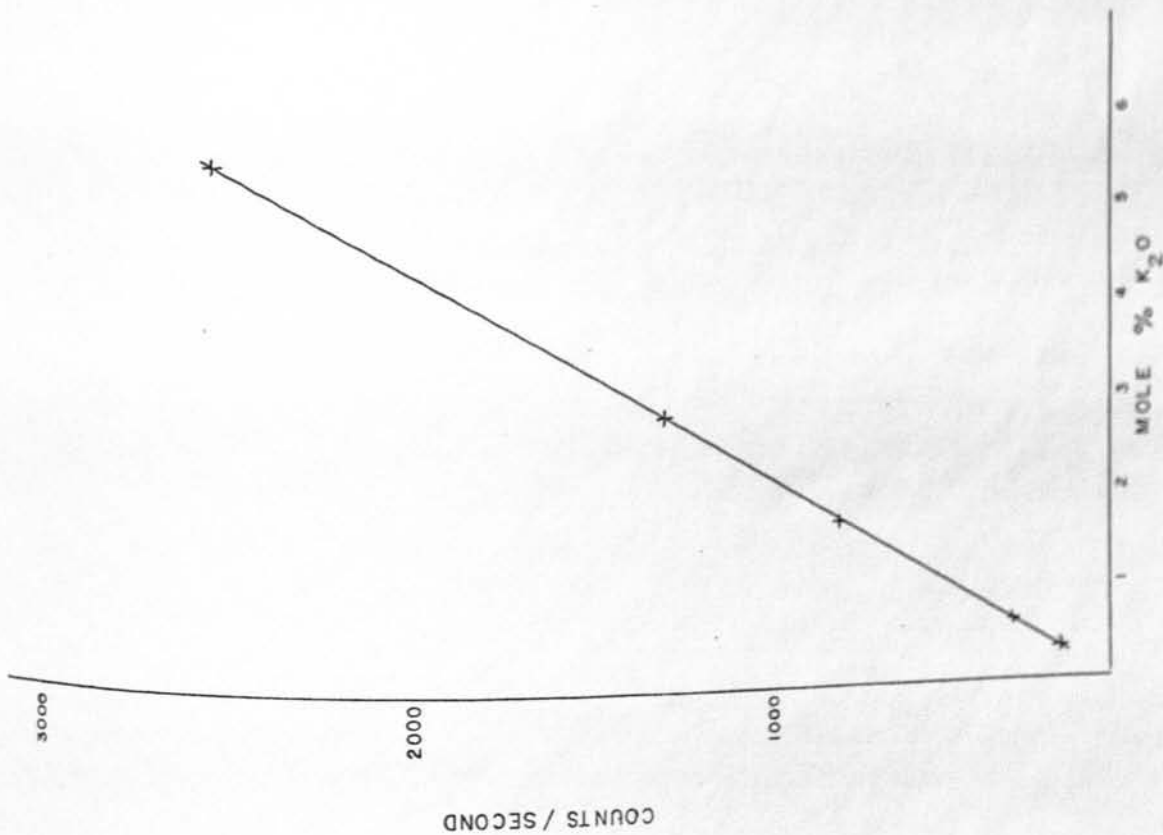


X-ray Tube Voltage = 50 KV  
X-ray Tube Amperage = 50 MA  
PHS Voltage = 1.625  
PHS E = 6.0  
PHS E<sub>L</sub> = 2.0  
Preset Time = 100 Seconds  
2θ = 57.52

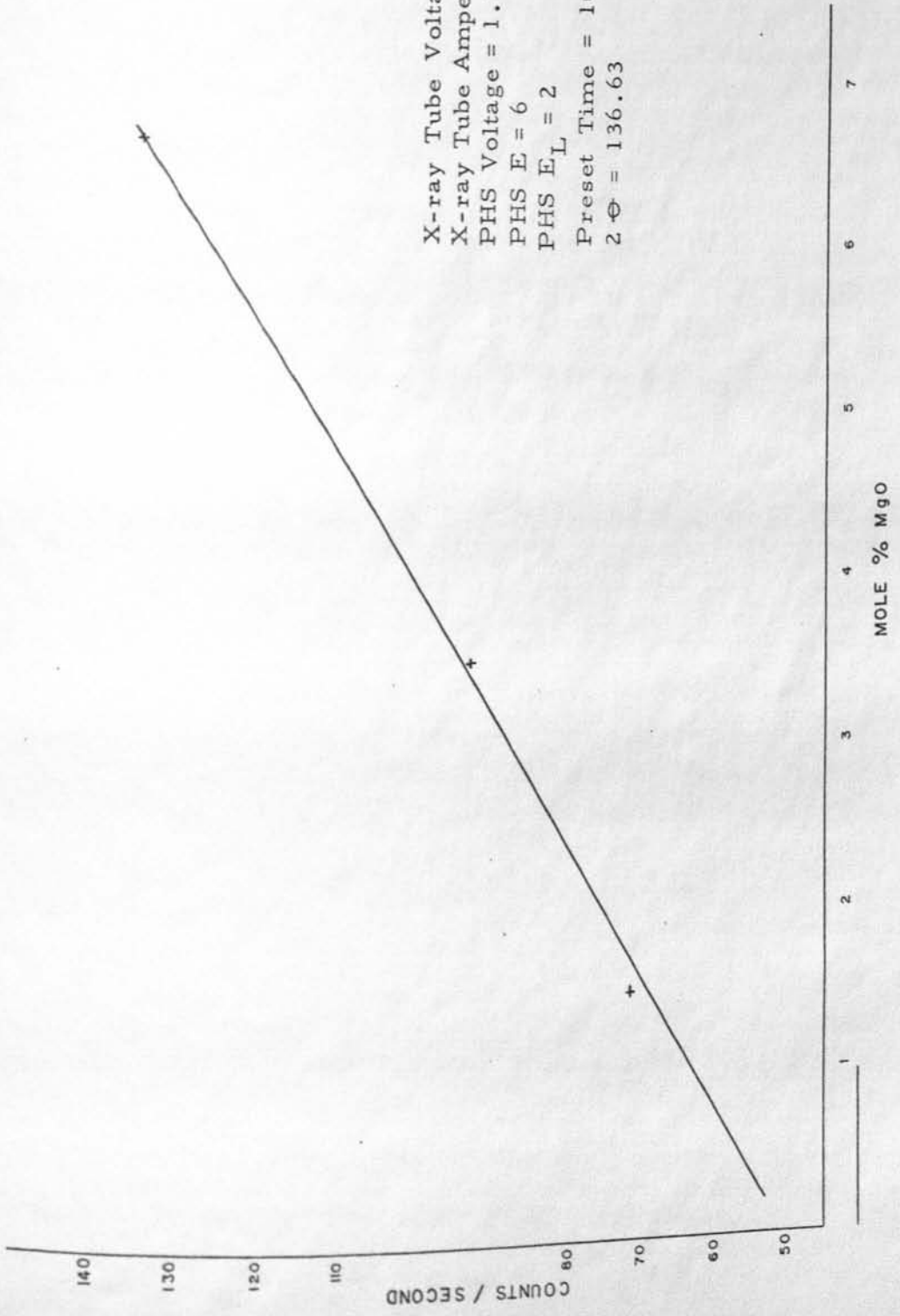


X-ray Tube Voltage = 50 KV  
X-ray Tube Amperage = 50 MA  
PHS Voltage = 1.625  
PHS E = 6  
PHS E<sub>L</sub> = 2

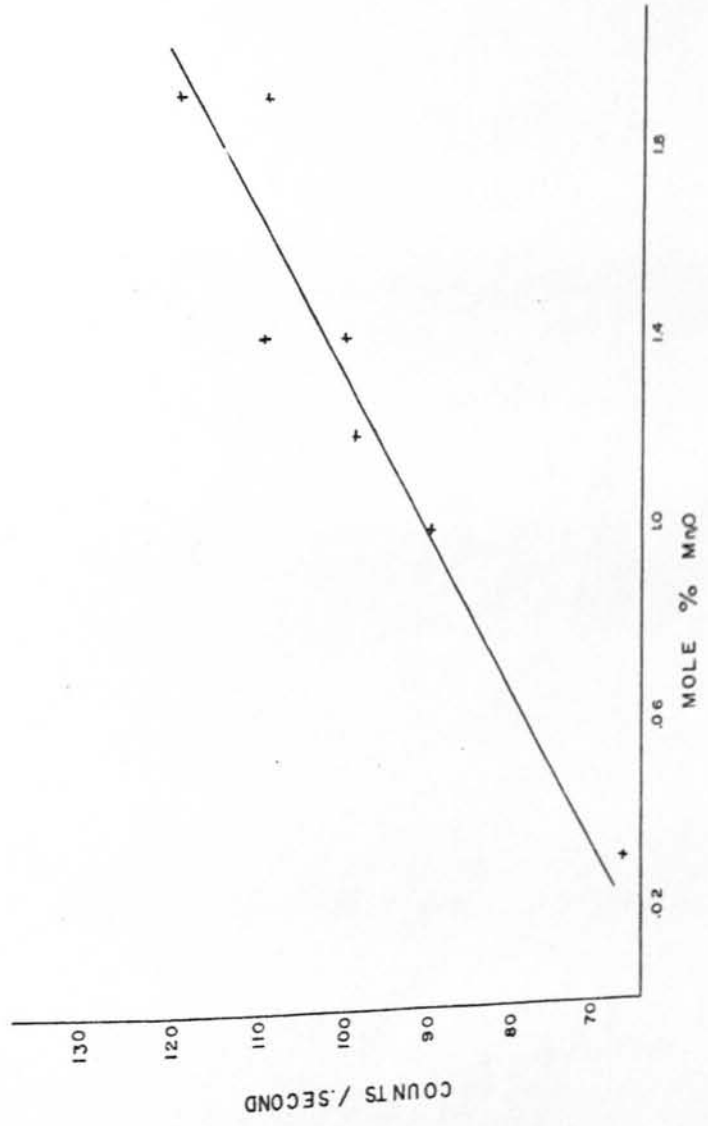
Preset Time = 100 Seconds  
2  $\theta$  = 50.46



X-ray Tube Voltage = 50 KV  
X-ray Tube Amperage = 50 MA  
PHS Voltage = 1.77  
PHS E = 6  
PHS E<sub>L</sub> = 2  
Preset Time = 1000 Seconds  
2- $\Theta$  = 136.63



X-ray Tube Voltage = 50 KV  
X-ray Tube Amperage = 50 MA  
PHS Voltage = 1.625  
PHS E = 6  
PHS E<sub>L</sub> = 2  
Preset Time = 100 Seconds  
2-Φ = 62.97



X-ray Tube Voltage = 50 KV  
X-ray Tube Amperage = 50 MA  
PHS E = 1.0  
PHS E<sub>L</sub> = 6.0  
Preset Time = 100 Seconds  
2θ = 109.06  
PHS Voltage = 1.825

